Effect of gold wire bonding process on angular correlated color temperature uniformity of white light-emitting diode

Bulong Wu,[1,2] Xiaobing Luo,[1,2,*] Huai Zheng,[2] and Sheng Liu[1,3]

[1]*Division of MoEMS, Wuhan National Laboratory for Optoelectronics, Wuhan, 430074, China*
[2]*School of Energy and Power Engineering, Huazhong University of Science and Technology, Wuhan, 430074, China*
[3]*School of Mechanical Science and Engineering, Huazhong University of Science and Technology, Wuhan 430074, China*
**luoxb@mail.hust.edu.cn*

Abstract: Gold wire bonding is an important packaging process of lighting emitting diode (LED). In this work, we studied the effect of gold wire bonding on the angular uniformity of correlated color temperature (CCT) in white LEDs whose phosphor layers were coated by freely dispersed coating process. Experimental study indicated that different gold wire bonding impacts the geometry of phosphor layer, and it results in different fluctuation trends of angular CCT at different spatial planes in one LED sample. It also results in various fluctuating amplitudes of angular CCT distributions at the same spatial plane for samples with different wire bonding angles. The gold wire bonding process has important impact on angular uniformity of CCT in LED package.

OCIS codes: (230.0230) Optical devices; (230.3670) Light-emitting diodes.

References and links

1. X. Luo, B. Wu, and S. Liu, "Effects of moist environments on LED module reliability," IEEE Trans. Device Mater. Reliab. **10**(2), 182–186 (2010).
2. B. P. Loh, P. S. Andrews, and N. W. Medendorp, "Light emitting device packages, light emitting diode packages and related methods," U.S. Patent 20,080,054,286 (Aug. 27, 2008).
3. G. H. Negley and M. Leung, "Methods of coating semiconductor light emitting elements by evaporating solvent from a suspension," U.S. Patent 7,217,583 (May 15, 2007).
4. G. O. Muller, R. G. Muller, M. R. Krames, P. J. Schmidt, H. H. Bechtel, J. Meyer, J. Graaf, and T. A. Kop, "Luminescent ceramics for a light emitting device," U.S. Patent 7,361,938 (Apr. 22, 2008).
5. B. Braune, K. Petersen, J. Strauss, P. Kromotis, and M. Kaempf, "A new wafer level coating technique to reduce the color distribution of LEDs," Proc. SPIE **6486**, 64860X (2007).
6. J. P. You, N. T. Tran, and F. G. Shi, "Light extraction enhanced white light-emitting diodes with multi-layered phosphor configuration," Opt. Express **18**(5), 5055–5060 (2010).
7. N. T. Tran and F. G. Shi, "Studies of phosphor concentration and thickness for phosphor-based white light-emitting-diodes," J. Lightwave Technol. **26**(21), 3556–3559 (2008).
8. Z. Y. Liu, S. Liu, K. Wang, and X. B. Luo, "Optical analysis of phosphor's location for high-power light emitting diodes," IEEE Trans. Device Mater. Reliab. **9**(1), 65–73 (2009).
9. C. Sommer, F.-P. Wenzl, P. Hartmann, P. Pachler, M. Schweighart, S. Tasch, and G. Leising, "Tailoring of the color conversion elements in phosphor-converted high-power LEDs by optical simulations," IEEE Photon. Technol. Lett. **20**(9), 739–741 (2008).
10. C. Sommer, F. P. Wenzl, F. Reil, J. R. Krenn, P. Hartmann, P. Pachler, and S. Tasch, "On the effect of light scattering in phosphor converted white light-emitting diodes," in *Solid-State and Organic Lighting*, OSA Technical Digest (CD) (Optical Society of America, 2010), paper SOTuB5
11. Y. Shuai, Y. Z. He, N. T. Tran, and F. G. Shi, "Angular CCT uniformity of phosphor converted white LEDs: effects of phosphor materials and packaging structures," IEEE Photon. Technol. Lett. **23**(3), 137–139 (2011).
12. R. Yu, S. Jin, S. Cen, and P. Liang, "Effect of the phosphor geometry on the luminous flux of phosphor-converted light-emitting diodes," IEEE Photon. Technol. Lett. **22**(23), 1765–1767 (2010).
13. K. Wang, D. Wu, F. Chen, Z. Y. Liu, X. B. Luo, and S. Liu, "Angular color uniformity enhancement of white light-emitting diodes integrated with freeform lenses," Opt. Lett. **35**(11), 1860–1862 (2010).
14. H. Zheng, J. L. Ma, X. B. Luo, and S. Liu, "Precise model of phosphor geometry by conventional dispensing in LEDs packaging," presented at the 12th International Conference on Electronic Packaging Technology & High Density Packaging, Shanghai, China, 8–11 Aug. 2011.

#154769 - $15.00 USD Received 16 Sep 2011; revised 23 Oct 2011; accepted 24 Oct 2011; published 10 Nov 2011

1. Introduction

As an energy saving light source, high bright white LED has been widely recognized to be the potential replacement for traditional general lighting source. In recent years, it has more and more applications in our daily life, such as road lighting, headlamps of automobiles, and backlighting for LCD display. So far, most of White LEDs (WLEDs) are based on phosphor-converted principle, in which a blue GaN LED is covered by a yellow phosphor made of YAG:Ce bound in silicone [1].

The major optical challenges for WLED are in terms of high light output efficiency and angular CCT uniformity. Phosphor coating technology is vital for the abovementioned challenges. To overcome the challenges, corporations such as Cree, Philips Lumileds, and Osram have developed various phosphor-dispersing technologies such as conformal coating, spinning coating and so on [2–5]. Except for the industrial development, a lot of simulation works have been conducted to study the influence of structures and parameters of phosphor layers on optical performances of WLEDs based on Monte Carlo ray tracing. Shi et al. used bi-layered phosphor method to package white LED and found this method caused more than 18% increase in luminous flux compared to conventional random mixed phosphor case at the same CCT [6], and they also investigated the dependence of luminous efficiency and CCT on phosphor concentration and thickness for WLEDs, and found that LED packaged with lower concentration and higher thickness phosphor had higher luminous efficiency [7]. Our group analyzed the effect of phosphor's location on LED packaging performance, and suggested an optical structure with plane and remote phosphor location should be a suitable choice for LED packaging with consideration of the luminous efficiency and color uniformity [8]. Sommer et al. also carried out simulations and pointed out phosphor concentration and the geometry size should be precisely adjusted to assure angular-homogeneous white light, and they also identify the impacts of different refractive indices and particle size of phosphor on CCT and luminous efficacies of WLEDs [9,10]. Some other studies on phosphor layer's geometry optimization are also conducted for the better performance of WLEDs [11,12].

In order to eliminate the inhomogeneity of angular color distribution in WLED with phosphor freely dispersed coating process, our group demonstrated a freeform lens to replace the traditional hemisphere silicone lens, and the angular color uniformity of WLED significantly increased from 0.334 to 0.957 [13].

Due to its simplicity and low cost, phosphor freely dispersed coating process is widely adopted in WLED production. For any phosphor coating methods as mentioned above, the electrical connection based on gold wire bonding is a must in LED packaging. However, the effect of gold wire bonding process on geometry of phosphor freely dispersed on LED chip, which ultimately affects WLED product's optical performance, is not considered by most researchers. So far, the LED manufacturers shorten the length of gold wire in order to cut down cost, and also neglect the effect of wire bonding on product performance. So it is necessary to study the impact of gold wire bonding process on angular CCT uniformity of this typical WLED package. In this paper, we will try to study the effect of gold wire bonding on the optical performance of LED by experiments.

2. Experimental processes

In this work, phosphor-converted WLEDs with freely dispersed phosphor coating are employed in study. Samples with different wire bonding angles were packaged. The experimental details are described as follows.

Firstly, one kind of 1 W conventional blue LED chips was used for the packaging. The chip is precisely bounded at the center of LED substrate. Secondly, electronic connections between LED chip and substrate are implemented by wire bonding. Four gold wires are bonded as the electronic connections, as shown in Fig. 1. Thirdly, phosphor gel, which was the mixture of YAG:Ce phosphor powder and silicone, is doped around LED chip freely to form phosphor layer as color converted element, as shown in Fig. 2. The mass concentration

#154769 - $15.00 USD Received 16 Sep 2011; revised 23 Oct 2011; accepted 24 Oct 2011; published 10 Nov 2011

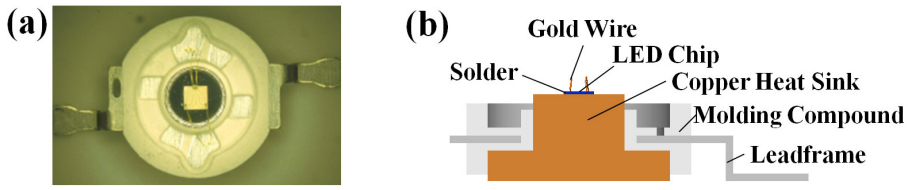

Fig. 1. LED module sample without phosphor layer: (a) top view; (b) sectional drawing at plane *C*0°–180°.

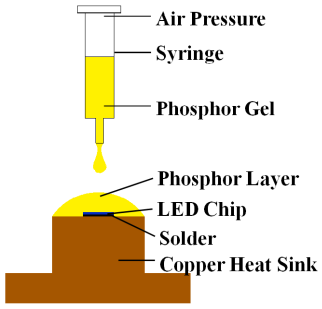

Fig. 2. Freely dispersed phosphor coating process.

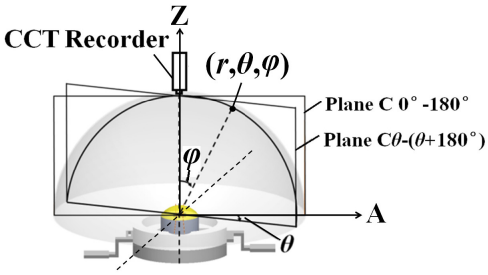

Fig. 3. Schematic of angular CCT measurement.

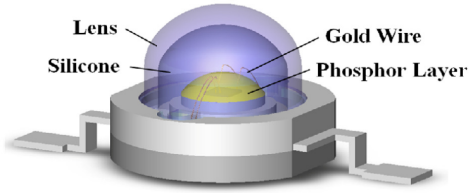

Fig. 4. Typical 1W LED package.

of phosphor powder was set at 13.04%. Fourthly, to cure phosphor gel, LED samples were placed in a vacuum baking chamber. Fifthly, the geometries of phosphor layers in LED samples were observed and their optical performances were measured. The sample's angular CCT at point (r,θ,φ) on plane $C\theta-(\theta+180°)$ of the top hemisphere is recorded as shown in Fig. 3. In Fig. 3, the point is specified by (r,θ,φ) in the coordinate system, where the origin is fixed at the center of top surface of copper heat sink; r is the radial distance; inclination angle φ is measured from the fixed zenith direction Z; azimuth angle θ is measured from azimuth axis A; Plane $C\theta-(\theta+180°)$ is defined as the plane passes origin and zenith direction Z, and azimuth angle of points on that plane is θ. During the process of CCT measurement, CCTs at points on plane $C0°-180°$ and plane $C90°-270°$ were measured, and r is set as a constant,

#154769 - $15.00 USD Received 16 Sep 2011; revised 23 Oct 2011; accepted 24 Oct 2011; published 10 Nov 2011

and inclination angle φ increases from $-90°$ to $90°$. Finally, the lens is laid on the substrate, and silicone gel is injected inside and forms the typical LED package, as shown in Fig. 4.

For the experiments, there are some notifications: a). LED chips with the same characteristics were selected for packaging sample; b). In order to study the impact of gold wires on the optical performance of LED samples, the gold wires were bounded to form different angles and shapes among LED samples.

3. Effect of wire bonding on geometry of phosphor layer

3.1 Modeling

For phosphor gel, surfaces of copper heat sink and gold wire are wettable. After gold wire bonding, the phosphor gel is freely doped on the LED chip on the round substrate. On the one hand, it spreads on the chip surface and top surface of copper heat sink in LED substrate; on the other hand, phosphor gel spreads over the wire surface. During the spreading process, phosphor gel will cover the wettable surfaces until reaching equilibrium state.

In the previous optical simulation of WLEDs, the gold wires are usually neglected and the phosphor layer is considered as a part of spherical cap. However, its real geometry, even without the impact of gold wires, is not exact truncated sphere, and it is closer to oblate spheroid, as shown in Fig. 5. For the LED samples, the phosphor gel morphology is mainly controlled by the surface tensions. A theory based on minimum free energy is applied to explain microfluidic morphology. Based on Laplace-Young equation, the precise model of phosphor layer geometry is built by our group [14].

Without the impact of gold wire, it is axially symmetric shape and its surface can be described as follows,

$$\gamma \frac{\frac{d^2 z}{dr^2}}{[1+(\frac{d^2 z}{dr^2})^2]^{\frac{1}{2}}} + \frac{\gamma}{r} \frac{\frac{dz}{dr}}{[1+(\frac{dz}{dr})^2]^{\frac{1}{2}}} = -\gamma K_0 + (\rho_l - \rho_g) g z \qquad (1)$$

where γ is the surface tension between liquid and gas; r and z are the radial and axial co-ordinate respectively; K_0 is the curvature of the interface of phosphor gel geometry at the edge of top surface in copper heat sink; ρ_l and ρ_g mean the densities of the liquid and gas respectively; g is the gravity acceleration. Although this second-order differential equation has no analytical solution, it can be solved by the numerical algorithm based on four-order Runge–Kutta method. Figure 6(a) shows the geometry shape of phosphor gel when not considering the gold wire based on the Eq. (1). It can be seen that the shape is not spherical cap.

In fact, the gold wires have important effect on the geometry of phosphor layer and it cannot be neglected. Due to wetting effect, the phosphor gel spreads along the gold wires' surfaces. In this case, the phosphor spreading process is complicated, but it can be simulated based on wetting theory. The shape of phosphor layer cannot be axially symmetric.

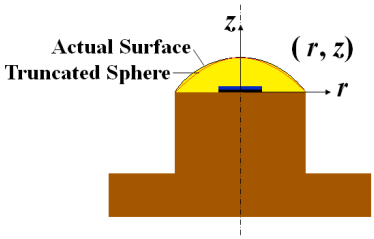

Fig. 5. Actual geometry of phosphor layer.

#154769 - $15.00 USD Received 16 Sep 2011; revised 23 Oct 2011; accepted 24 Oct 2011; published 10 Nov 2011

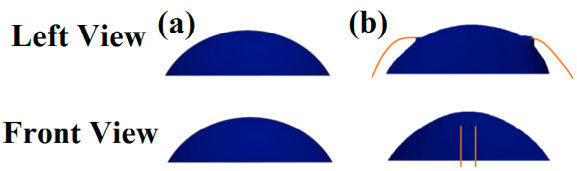

Fig. 6. Left and front views of phosphor layers in LED modules: (a) without gold wires; (b) with gold wires.

Based on the flow simulation, we also obtained the phosphor layer shapes at the cases with the gold wire, as shown in Fig. 6(b). From Fig. 6(b), we can see that the geometry of phosphor layer with considering gold wires is not axially symmetric. The effect of gold wire on the phosphor gel shape is existed.

3.2 Experimental observation and comparison

The left and front views of gold wires and phosphor layers in five test samples are shown in Fig. 7. It can be seen that experimental observation proves the calculation results shown in Fig. 6. The shape of phosphor is not axially symmetric. Thus, it is expected that this will result in the nonuniformity of optical performance in the package, especially CCT deviation.

Figure 8 schematically shows the gold wire shapes and heights in the five samples from the left view. According to the experimental results shown in Fig. 7, the profiles of phosphor layers influenced by the gold wires are also depicted in Fig. 8. It indicates that various gold wire shapes and heights result in different phosphor layer geometries. Compared with the phosphor layer without considering gold wires, it is clear that the shapes of phosphor layers in sample 2, sample 3 and sample 5 are influenced by gold wires seriously, especially at where the gold wires locate. In sample 3, the gold wires are lower than that in sample 1, and the external part is closer to the surface of phosphor, more phosphor gel spreads along gold wires surfaces until surface energy among air, phosphor gel and surface of gold wire becomes balanced. Obviously, this will reduce the height of phosphor layer and change its curvature. For sample 1 and sample 4, the gold wires' effect on phosphor layer geometry is tiny, and the left and front views of phosphor layers are nearly the same.

To prove the effect of different geometries on the optical performance of WLED, it is necessary to conduct some optical tests on these samples.

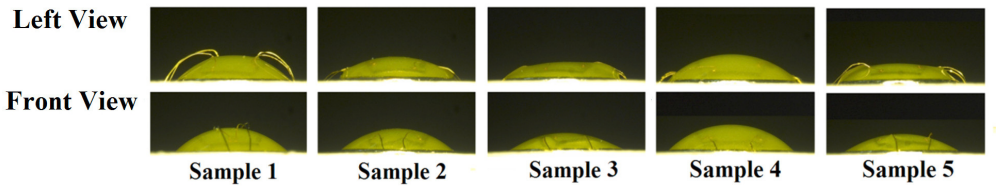

Fig. 7. Left and front views of phosphor layers in LED module samples.

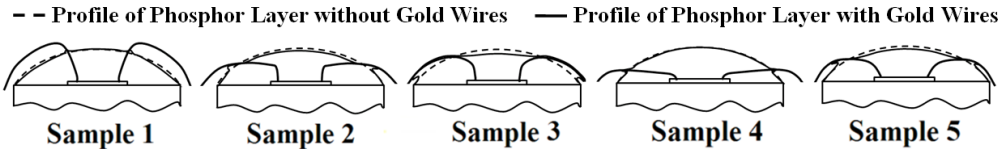

Fig. 8. Gold wires shape and height of the five samples and phosphor profile.

4. Optical test results and discussions

Usually, one constant value of CCT is given by integrating sphere optical measurement system for one LED package. Here, CCTs of sample 1, sample 2 and sample 3 and CCTs of sample 4 and sample 5 belong to different ranges $(5500K-6500K)$ and $(4500K-5500K)$,

#154769 - $15.00 USD Received 16 Sep 2011; revised 23 Oct 2011; accepted 24 Oct 2011; published 10 Nov 2011

respectively. Therefore we put samples 1 to 3 into Fig. 9(a) and samples 4 to 5 into Fig. 9(b). The constant value of CCT is not enough to evaluate the package's optical performance accurately, because the spatial angular CCT in one LED package is not a constant value.

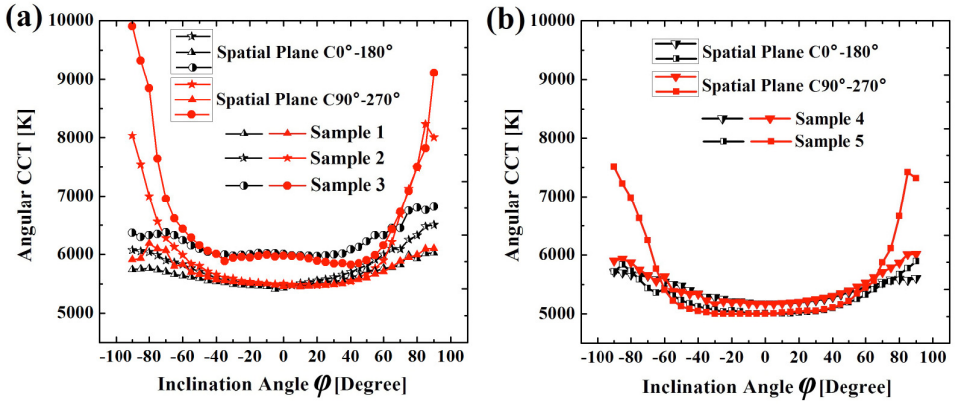

Fig. 9. Angular CCT distributions at plane $C0°$–$180°$ and plane $C90°$–$270°$: (a) sample 1, sample 2 and sample 3; (b) sample 4 and sample 5.

Figure 9 shows the measurement results of spatial angular CCT distributions of different samples, detected by CCT recorder. As shown in Fig. 9, for all the samples, the angular CCT fluctuation at plane $C0°\text{-}180°$ is smaller than that at plane $C90°\text{-}270°$ in the package. This is due to that the geometries of phosphor layers at plane $C90°\text{-}270°$ in all the samples are affected by gold wires more seriously than that at plane $C0°\text{-}180°$, as shown in Fig. 7. Taking sample 5 for instance, the angular CCT decreases dramatically from 7512 K (at $\varphi = -90°$) to 5050 K (at $\varphi = -40°$) at plane $C90°\text{-}270°$, while it decreases from 5719 K (at $\varphi = -90°$) to 5125 K (at $\varphi = -40°$) at plane $C0°\text{-}180°$.

It also can be found that for sample 1 and sample 4, the angular CCT distributions, are similar at plane $C0°\text{-}180°$ and plane $C90°\text{-}270°$, whereas, for sample 2, sample 3 and sample 5, angular CCT deviates from each other sharply when inclination angle φ changes from $0°$ to $\pm 90°$ at the two planes. This is because the phosphor gel shapes at the two planes vary less for sample 1 and sample 4, as we mentioned in Fig. 7.

At the same spatial plane $C90°\text{-}270°$, fluctuating amplitudes of CCT distributions are also different for samples with different wire bonding shapes. Figure 10 shows the angular CCT distributions of sample 1 and sample 3 at the plane $C90°\text{-}270°$. When inclination angle

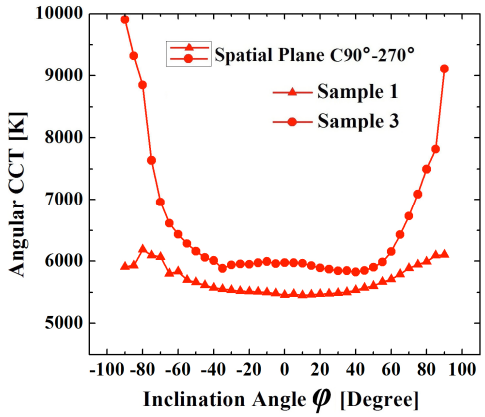

Fig. 10. Angular CCT distributions of sample 1 and sample 3 at plane $C90°$–$270°$.

#154769 - $15.00 USD Received 16 Sep 2011; revised 23 Oct 2011; accepted 24 Oct 2011; published 10 Nov 2011

φ increases from −90° to 0° , angular CCT of sample 3 changes from 9904 K to 5976 K, while it changes from 5801 K to 5457 K for sample 1. The fluctuating amplitude of sample 3 is much larger than that of sample 1. This can be explained through the left views of these two samples in Fig. 7. The phosphor gel soaks the surfaces of gold wires apparently and its geometry is influenced more seriously in sample 3, compared with sample 1.

All these experimental results about angular CCT distributions correspond well with the geometries of phosphor layers. The CCT distributions of LED modules, encapsulated with silicone gel and lens, also indicate the similar trend. It illustrates that the gold wire bonding process has an important impact on angular CCT distribution of LED package.

5. Summary

In summary, the effect of gold wire bonding process on the angular uniformity of CCT in WLEDs was analyzed. The experimental study indicated that the gold wire bonding impacts the geometry of phosphor layer distinctly. This induces the different fluctuation trends of angular CCT at different spatial planes in the LED package and results in various fluctuating amplitudes at the same spatial plane for samples with different wire bonding shapes and heights. Thus, during the manufacturing process of LED products, the gold wire shape should be well designed and optimized in order to improve the optical performance of products.

Acknowledgments

This work was supported in part by National Natural Science Foundation of China (NSFC) Project under grant number 50876038, in part by Ph.D. Programs Foundation of Ministry of Education of China under grant number 20100142110046 and in part by New Century Excellent Talents Project of Chinese Education Ministry under contract number NCET-09-0387.

#154769 - $15.00 USD Received 16 Sep 2011; revised 23 Oct 2011; accepted 24 Oct 2011; published 10 Nov 2011